

Diurnally Varying Wind Forcing and Upper Ocean Temperature: Implications for the Ocean Mixed Layer

Sarah T. Gille

Scripps Institution of Oceanography and Department of Mechanical and Aerospace Engineering, University of California, San Diego

Abstract. Solar radiation varies on a diurnal cycle, and therefore so do all the climate variables that it forces, including sea surface temperature (SST), wind, and in turn mixed-layer depth and upper-ocean heat storage. Satellite scatterometer data from the QuikSCAT and ADEOS-2 tandem mission have been used to estimate the amplitude and phasing of diurnal wind variations on a global basis. Statistically significant diurnal wind variations occur along coastlines all over the world, where they are commonly thought of as the land/sea breeze. Open ocean winds also undergo substantial diurnal variability at latitudes equatorward of 30° latitude. The phasing of diurnal winds varies with distance from the shore. Upper ocean temperatures measured from profiling Argo floats are compared with microwave SSTs from the Advanced Microwave Scanning Radiometer for the Earth Observing System (AMSR-E) to estimate the amplitude and phasing of the diurnal cycle in upper ocean temperature. Differences between Argo and AMSR-E measurements imply that the diurnal cycle has an amplitude that decreases with increasing latitude, from about 0.1°C near the equator to 0.02°C near 60°N/S. Maximum upper ocean temperatures occur around 18:00 local time at most latitudes. If only temperature or only wind underwent a diurnal cycle, then over the course of the day, the variations would average to zero, and we would expect no net impact on climate. Since the two processes both vary, with different phasings, they are expected to have a combined (rectified) effect on the mixed-layer, and this effect is evaluated.

1. Introduction

Solar radiative forcing of the Earth varies on a 24-hour cycle, and this diurnal periodicity is a fundamental character of the Earth's climate system. Diurnal solar forcing translates into diurnal variations in winds, particularly equatorward of 30° latitude [e.g. Walsh, 1974; Niino, 1987; Gille et al., 2005] and diurnal variations in upper ocean temperature [e.g. Donlon et al., 2007].

Diurnal variability is challenging to measure from satellite, because many Earth-orbiting satellites are launched on sun synchronous orbits, meaning that they sample at roughly the same local time on each ascending (northward) and descending (southward) satellite pass. Sun synchronous orbits offer engineering design advantages, because no action is required in order to maintain the same orientation of solar panels relative to the sun for each satellite pass, and sun angle corrections are the same for each satellite pass. However sun synchronous orbits have the distinct disadvantage of sampling at the Nyquist frequency of the diurnal cycle.

This study explores two strategies for evaluating diurnal variability using data from sun synchronous satellites. For scatterometer wind data, the diurnal cycle can be studied for a six month period in 2003 corresponding to the QuikSCAT and ADEOS-2 tandem

mission. For microwave sea surface temperatures, the diurnal cycle can be evaluated by comparing sea surface temperatures measured by the Advanced Microwave Scanning Radiometer (AMSR-E) with upper ocean temperatures measured by profiling Argo floats.

Diurnal variability in wind and sea surface temperature do not appear to have consistent timing everywhere. While sea surface temperature follows a fairly consistent diurnal cycle, with maximum temperatures in mid to late afternoon, diurnal winds vary with distance from the coast. The final part of this study explores the impact of this effect on ocean mixed-layer depth.

2. Diurnal Winds

The SeaWinds scatterometers aboard QuikSCAT and ADEOS-2 measure wind speed and direction with roughly 25 km resolution. QuikSCAT, launched in 1999, has equatorial overpass times of 6 am and 6 pm. The ADEOS-2 satellite, which flew for six months from April through October 2003, crossed the equator at 10:30 am and 10:30 pm. Gille et al. [2003] made use of the QuikSCAT morning–evening wind differences to assess the basic characteristics of diurnal wind variability. Gille et al. [2005] used the four measurements per data collected from the QuikSCAT and ADEOS-2 tandem mission to consider how winds rotate along an elliptical hodograph through the course of the diurnal cycle. Figure 1 shows that the amplitude of the diurnal wind stress varies substantially depending on location, with strong diurnal winds near coastlines and elevated diurnal amplitudes typically near large orographic features. Statistically significant diurnal variability occurs throughout the tropics [Gille et al., 2005]. As reported by Gille et al. [2005], these global findings are generally consistent with linear theory [Alpert et al., 1984].

The timing of the maximum wind, shown in Figure 2, changes with location. Near coastlines there is evidence that maximum winds propagate offshore progressively through the course of the day. Within the tropics, the time of maximum wind varies progressively across the Pacific Ocean [Gille et al., 2005].

3. Diurnal Upper Ocean Temperatures

Compared with diurnal wind variability, diurnal cycles in sea surface temperature are harder to extract from satellite data, because the radiative properties of the lower atmosphere could change on a diurnal cycle, thus providing different biases for daytime and nighttime sea surface temperature calibration data. In order to evaluate the diurnal variations in upper ocean temperatures, AMSR-E SSTs were compared with co-located upper ocean temperatures measured at 5 m depth (T_{5m}) by profiling Argo floats. AMSR-E (launched in 2002) measures temperature at 1:30 am and 1:30 pm local time. In contrast, Argo floats (which achieved global coverage roughly starting in 2002) rise to the surface throughout the course of a 24-hour cycle, and are therefore able to measure T_{5m} at all times of day. For these comparisons, daytime and nighttime AMSR-E data were treated separately. Co-located AMSR-E and Argo data pairs were sorted based on the time separation between measurements and bin averaged based on time separation. Since AMSR-E measurements occur within a narrow window in local time, the time variability

comes from the Argo sampling. Figure 3 shows mean temperature differences obtained by subtracting AMSR-E SSTs from Argo T_{5m} . Both daytime and nighttime AMSR-E data imply comparable diurnal cycles. Nighttime temperatures tend to be colder than Argo measurements, while daytime AMSR-E measurements are warmer than most of the Argo measurements. Warmest temperatures appear to occur a few hours after the satellite overpass time, roughly around 6 pm.

The amplitude of the diurnal cycle varies with latitude (Figure 4) and is strongest near the equator. At higher latitudes, it is detectable in the summer but can be indistinguishable from zero in the winter, as indicated by the differences between the two panels of Figure 4. The phasing of the diurnal cycle is relatively constant at all latitudes where the amplitude is distinct from zero, as illustrated in Figure 5.

4. Implications for the Mixed Layer

The results presented here provide an incomplete picture of the geographic variations in wind and SST diurnal cycles. However, they seem to suggest that SST, like solar radiative forcing, is likely to have a fairly constant phasing, while wind patterns can vary substantially with distance from the coast. This has potentially significant impact on the depth of the ocean mixed layer.

The mixed layer is the region of the upper ocean that is vertically homogenized, so that all water feels the effects of the atmosphere. It has important implications for climate, because it determines how heat is transmitted between the atmosphere and the upper ocean. The mixed layer depth depends on wind forcing, upper ocean temperature profiles and surface heat fluxes. Because of the diurnal cycle in radiative forcing, the mixed layer depth necessarily undergoes a diurnal cycle, as demonstrated by the model of Price et al. [1986] (henceforth PWP).

If surface wind stress also varies with a diurnal periodicity, that may further modify the mixed layer depth. To test that effect, the PWP model was run with diurnally varying winds, with a mean of 0.05 N m^{-2} and diurnal amplitude of 0.02 N m^{-2} with varying phase. Results for a tropical test case in Figure 6 show that the mixed layer undergoes a diurnal cycle, with a minimum depth during the day regardless of the timing of the wind. The mixed-layer deepens progressively through the afternoon and evening, and the exact timing of the deepening, as well as the maximum depth of the mixed layer, both vary depending on the timing of the wind relative to the radiative forcing.

Here, a wind phase of 0 implies strong winds at midnight, and a wind phase of 0.5 implies strong daytime winds. Winds that peak during the daytime result in more rapid deepening of the mixed layer as the lines corresponding to different wind phasing indicate

in Figure 6. On average, daytime winds result in deeper mixed layers, as shown in Figure 7. When the diurnal cycle is strong compared to the mean winds, as is the case for the blue curve in Figure 7, this distinction can be dramatic and may have a significant impact on the mean depth and heat content of the mixed layer.

5. Summary and Conclusions

A single sun synchronous satellite is insufficient to extract the full diurnal cycle. Here the diurnal cycle in wind is extracted using data from the QuikSCAT and ADEOS-2 tandem scatterometer mission and the diurnal cycle in upper ocean temperature is estimated by comparing AMSR-E SST data with near surface temperatures collected by Argo profilers. Both wind and ocean temperatures have maximum diurnal cycles in summer. Results suggest that the phasing of wind may not uniformly coincide with the phasing of SST or radiative forcing. The implications of this phasing discrepancy are investigated using the PWP model, and results suggest that mixed layers are likely to be deeper in geographic regions where winds reach their maximum speed during the day.

Acknowledgments. This work was supported by NASA contract NNX08AI82G.

References

- Alpert, P., M. Kusuda, and N. Abe, 1984: Anticlockwise rotation, eccentricity and tilt angle of the wind hodograph. Part II: An observational study. *J. Atmos. Sci.*, **41**(24), 3568–3583.
- Donlon, C., I. Robinson, et al., 2007: The global ocean data assimilation experiment high-resolution sea surface temperature pilot project. *Bull. Am. Met. Soc.*, **88**, 1197–1213.
- Gille, S. T., S. G. Llewellyn Smith, and S. M. Lee, 2003: Measuring the sea breeze from QuikSCAT scatterometry. *Geophys. Res. Lett.*, **30**. 10.1029/2002GL016230.
- Gille, S. T., S. G. Llewellyn Smith, and N. M. Statom, 2005: Global observations of the land breeze. *Geophys. Res. Lett.*, **32**(5). L05605 10.1029/2004GL022139.
- Niino, H., 1987: The linear theory of land and sea breeze circulation. *J. Meteorol. Soc. Japan*, **65**, 901–921.
- Price, J. F., R. A. Weller, and R. Pinkel, 1986: Diurnal cycling: Observations and models of the upper ocean response to diurnal heating, cooling, and wind mixing. *J. Geophys. Res.*, **91**, 8411–8427.
- Walsh, J. E., 1974: Sea breeze theory and applications. *J. Atmos. Sci.*, **31**, 2012–2026.

Sarah T. Gille, Scripps Institution of Oceanography, University of California San Diego, La Jolla, CA 92093-0230 (sgille@ucsd.edu)

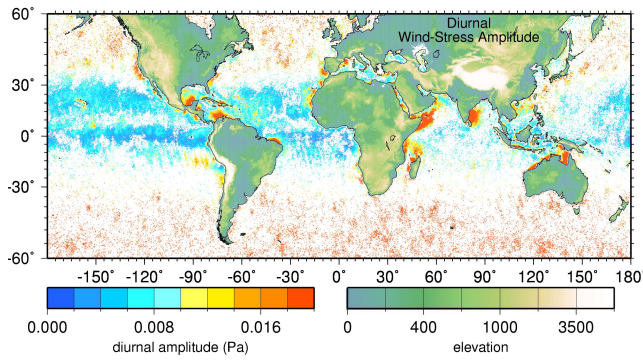


Figure 1. Strength of diurnal wind cycle, with major axis plotted in color in locations where it is statistically significant. Adapted from Gille et al. [2005].

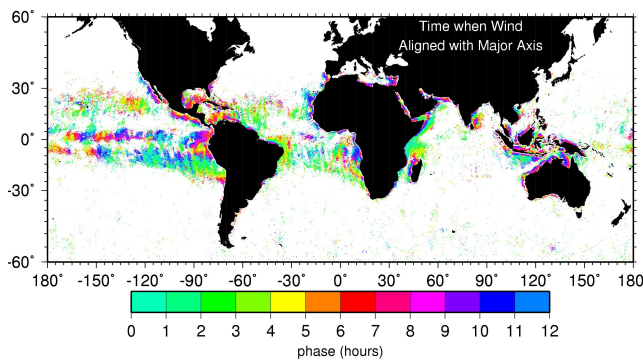


Figure 2. Time of day when wind is aligned with major axis. (Winds are aligned with the major axis twice a day.) Adapted from Gille et al. [2005].

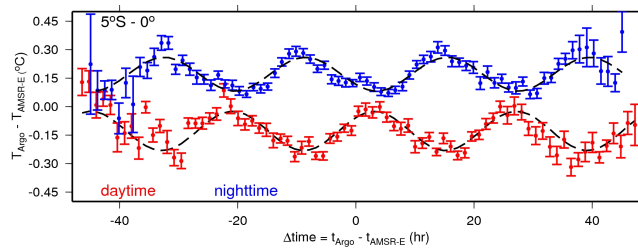


Figure 3. Temperature difference between co-located Argo T_{5m} and AMSR-E SST, as a function of time separation between observations for the latitude range between 5°S and the equator. Comparisons with daytime AMSR-E observations are in red and comparisons with nighttime AMSR-E observations in blue.

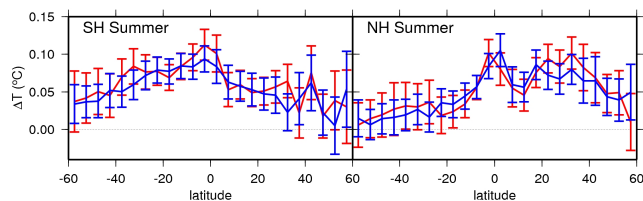


Figure 4. Amplitude of diurnal temperature cycle, plotted as a function of latitude for daytime (red) and nighttime (blue). Southern Hemisphere summer data (i.e. Northern Hemisphere winter) are plotted on the left and Northern Hemisphere on the right. Here amplitude is determined from a sinusoidal fit to the bin-averaged observations.

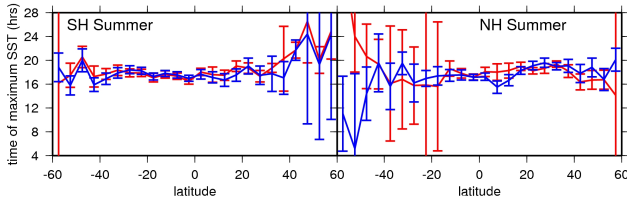


Figure 5. Time of maximum temperature, determined from a sinusoidal fit to AMSR-E minus Argo temperature observations for daytime (red) and nighttime (blue). Data are segregated by season as in Figure 4

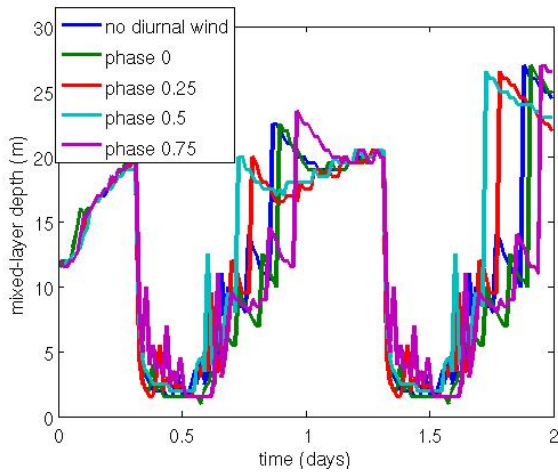


Figure 6. Mixed-layer depth as a function of time as determined using the PWP model run over a two day period. Here the mean wind stress is 0.05 N m^{-2} , and the diurnal winds vary sinusoidally with an amplitude of 0.02 N m^{-2} . Colored lines indicate the phase of the diurnal cycle relative to the diurnal surface heat flux. A phase of 0.5 implies that wind reaches a maximum when the heat flux is maximum.

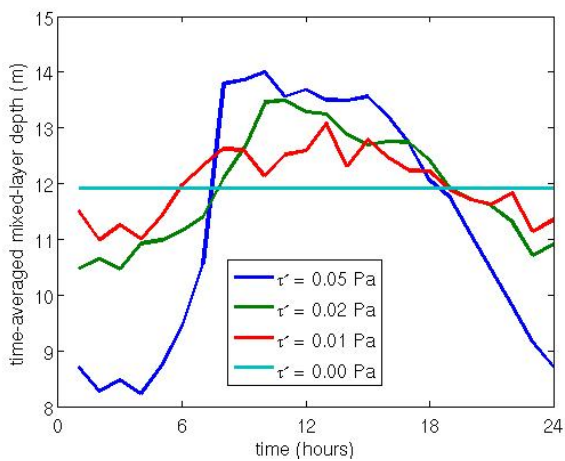


Figure 7. Mixed-layer depth as a function of phase lag of wind relative to radiative forcing. Here a phase of 12 hours implies that wind and radiative forcing are both at a maximum around noon. Different lines show results for different amplitudes of the diurnal cycle relative to a mean of 0.05 N m^{-2} .